Configuration Interaction Study of the Low-Lying Electronic States of GaBi

Anjan Chattopadhyay, Surya Chattopadhyaya, and Kalyan Kumar Das*

Department of Chemistry, Physical Chemistry Section, Jadavpur University, Kolkata 700 032, India

Received: September 20, 2001; In Final Form: January 7, 2002

Ab initio based multireference singles and doubles configuration interaction calculations, which include relativistic effective core potentials of the constituting atoms, have been carried out to study the low-lying electronic states of GaBi. Potential energy curves and spectroscopic constants of the electronic states within 46 000 cm^{-1} of energy have been reported. The ground-state dissociation energy of GaBi is calculated to be 1.24 eV as compared with the observed value of 1.60 ± 0.17 eV. Effects of the spin−orbit coupling on the spectroscopic properties of some low-lying states below 25 000 cm^{-1} have been studied. A large spin−orbit coupling produces a strong mixing among different Λ-S states and changes the characteristics of the potential energy curves. Several avoided crossings in the potential curves of Ω states of GaBi are also noted. The zero-field splitting of the ground state of GaBi is estimated to be 463 cm^{-1}. The $A^3\Pi-X^3\Sigma^-$ transition has been predicted to be quite strong. Three other transitions, namely, $A^3\Pi-{}^3\Pi$, $2^1\Sigma^+-{}^1\Pi$, and $2^1\Sigma^+-{}^1\Sigma^+$ are also studied. A few transitions from the $A^3\Pi_{0^+}$ component, which survives the predissociation, are reported to be highly probable. The radiative lifetime of $A^3\Pi_{0^+}$ is estimated, and the component is found to be short-lived. The oscillator strengths of 0^+-0^+ and 0^+-1 transitions for the lowest few vibrational levels are reported. A comparison of the electronic spectrum of GaX(X = P, As, Sb, Bi) molecules has been made.

I. Introduction

Experimental as well as theoretical research[1−38] on semiconductor molecules and clusters of group III and V elements are being persued over the past few decades because of their technological importance. Especially, molecules such as GaP, GaAs, GaSb, etc. and their neutral and ionic clusters are used as semiconductors in the preparation of electronic devices. The indium isomers of these compounds are also useful materials for the same purpose. Smalley and co-workers[1−6] have made pioneering work on the clusters of gallium arsenide. The follow-up investigations on the electronic structure and spectroscopic features have been also carried out by these authors using laser photoionization and the time-of-flight mass spectrometry measurement techniques. The jet-cooled GaAs has been studied by the resonant two-photon ionization spectroscopy.[7] Neumark and co-workers[8−12] have used the negative ion zero-electron kinetic photodetachment spectroscopic techniques to study the electronic states of the neutral group IV and group III−V clusters. Weltner and co-workers[13−15] have studied matrix-isolated electron-spin-resonance (ESR) spectra of small clusters of Ga, Si, Sn, and mixed group III−V elements. By using laser vaporization techniques, the infrared absorption spectra of GaX and InX (X= P, As, Sb) molecules in rare-gas matrices have been observed by Li et al.[15,16] Although a large number of studies have been reported for the electronic structure and spectroscopic properties of GaAs, there seems to have a very little data on the isovalent GaBi molecule. The mass spectrometric investigation of GaBi has been performed by Piacente and Desideri.[17] The dissociation energy of the GaBi molecule has been evaluated considering the process GaBi(g) → Ga(g) + Bi(g). The most probable experimentally determined value of the dissociation energy of GaBi is reported to be D_0^0(GaBi) = 37 ± 4 kcal $mole^{-1}$. Similar investigations on TlAs, TlBi, and Sn_2 molecules have been also made by these authors.

Theoretical studies on the spectroscopic properties and electronic structure of molecules of group III and V are being carried out in recent years. Balasubramanian and co-workers[18−28] have performed large-scale configuration interaction (CI) calculations using several methods such as complete active space self-consistent field (CASSCF)/CI, first order, second order, and multireference CI on several diatomic and triatomic molecules, and ions of group III and V elements. These calculations have included relativistic effects through the effective core potentials. Relativistic effects on molecules and clusters have been reviewed recently by Balasubramanian.[22,23] Potential energy curves and spectroscopic properties of several trimers such as $InAs_2$, $SbIn_2$, $GaAs_2$, $AsGa_2$, etc. in their low-lying electronic states have been calculated by Das and Balasubramanian.[24] The phosphides of gallium and indium in their mixed isomeric forms have been studied by Feng and Balasubramanian[25−28] using CI calculations at different levels. Meier et al.[29] have performed large-scale CI calculations on the low-lying electronic states of AlP. The local spin density method has been used by Russo and co-workers[30−32] to study the electronic states of CuIn, AgIn, CuGa, AgGa, etc. and clusters. The phosphides of arsenic and antimony are also studied in a similar set of calculations. In recent years, ab initio based multireference singles and doubles CI (MRDCI) calculations on the electronic spectrum of diatomic molecules of group III and V have been carried out by Das and co-workers.[33−38] Systematic studies on the low-lying electronic states of GaX and InX (X= P, As, Sb) have revealed the existence of the $A^3\Pi-X\ {}^3\Sigma^-$ bands, which are strong enough to be observed experimentally. However, only for GaAs, the A−X band has been observed in the gas phase so far. Lemire et al.[7] have observed the predissociations of the $A^3\Pi_{2,1,0^-}$ components of GaAs, whereas the $A^3\Pi_{0^+}$ component is found to be stable and undergoes transitions to the ground-state

* To whom correspondence should be addressed. E-mail: kalyankd@hotmail.com. das_kalyank@yahoo.com.

10.1021/jp013582v CCC: $22.00
Published on Web 02/16/2002

components. Recent CI calculations[33,35] predict similar predissociations for the $\Omega = 2$, 1, and 0^- components of the $A^3\Pi$ states of the isovalent GaP and GaSb molecules. There exists no theoretical or experimental data for the electronic structure and spectroscopic features of the isovalent GaBi molecule.

This paper is aimed at the theoretical studies of the potential energy curves and spectroscopic properties of low-lying electronic states of the GaBi molecule by using the MRDCI method, which uses relativistic effective core potentials (RECP) of Ga and Bi atoms and their spin−orbit coupling. Because the molecule is considerably heavy, one may expect comparatively strong spin−orbit effects on the spectroscopic parameters. In this connection transition probabilities of several spin-forbidden transitions are estimated in the present study. A special emphasis is given on the A−X transition, which is strongly probable for all group III−V diatomic molecules. The estimation of radiative lifetimes of excited states is also the subject of the present study.

II. Details of Computations

In the present calculations, $3d^{10}4s^24p$ electrons of Ga and $5d^{10}6s^26p^3$ electrons of Bi have been kept in the valence space, whereas the remaining electrons are substituted by the semicore RECP available in the literature. The RECP of the gallium atom are taken from Hurley et al.,[39] whereas for Bi, RECP of Wildman et al.[40] have been used. This essentially reduces the number of active electrons in our calculations. The primitive Gaussian basis functions of the type (3s3p4d) for Ga, taken from Hurley et al.,[39] are augmented with an additional d-polarization function of the exponent 0.207 a_0^{-2}. However, the first two d functions are contracted so that the final basis set of Ga becomes (3s3p5d/3s3p4d). For the bismuth atom, the (6s6p6d) basis set of Wildman et al.[40] is used with the first two d functions being contracted. Basis sets of both the atoms are compatible with their corresponding RECP and sufficient enough to describe the atomic orbitals accurately. Using these pseudopotentials and basis sets, a set of SCF molecular orbital (MO) calculations has been carried out at each internuclear distance for the $...\pi^2\ ^3\Sigma^-$ state of GaBi having 28 valence electrons. To perform CI calculations, we have used 90 optimized symmetry adapted SCF-MOs as basis functions. When the compositions of SCF-MOs are analyzed, it is noted that 20 d electrons of Ga and Bi remain localized on to their 3d and 5d orbitals, respectively. These electrons do not participate in the formation of the Ga−Bi bond in low-lying excited states. Therefore, 20 d electrons are essentially kept frozen, whereas only eight active electrons are used for the generation of configurations in the CI space.

The present computations are based on the MRDCI codes of Buenker and co-workers.[41−46] In the first step of the calculations, Λ-S states are studied without considering any spin−orbit interaction. The actual computations have been carried out in the C_{2v} subgroup of $C_{\infty v}$ in which the GaBi molecule belongs. The molecule has been placed along the $+z$ axis with Ga at the origin. The lowest eight roots for each irreducible representation of a given spin multiplicity are optimized in the CI step. We are confined here with singlet, triplet, and quintet spin states of GaBi. The low-lying excited Λ-S states in a given symmetry are defined by a set of main reference configurations. The singly and doubly excited configurations are generated from these reference sets. The sizes of the generated CI space for a given symmetry easily exceed a million in number. However, a configuration-selection procedure has been used to reduce the dimension of the eigenvalue problem. In the present calculations, a configuration-selection threshold of 1.0 μhartree has been used so that the sum of the squares of coefficients of the reference configurations for each root remains above 0.90. Therefore, the configuration-selection procedure reduces the number of the secular equations in the CI space to a large extent without losing much accuracy in the calculations. The energy extrapolation technique along with Davidson correction,[47,48] which takes care of higher excitations, gives an accurate estimate of the full-CI energy. The calculations have been carried out at a series of bond distances from 3.0 to 15.0 a_0 with different increments ranging between 0.05 and 5.0 a_0. Potential energy curves of a few lowest roots of each Λ-S symmetry are obtained from the estimated full-CI energies. The property matrix elements are, therefore, computed from the symmetry adapted CI wave functions.

In the second stage of calculations, the spin−orbit operators of Ga and Bi are taken from Hurley et al.[39] and Wildman et al.,[40] respectively, for the inclusion of the spin−orbit coupling in the calculations. The Λ-S CI wave functions are used as a basis for the spin−orbit calculations, which have been carried out in the $C_{2v}{}^2$ group representations, namely, A_1, A_2, and B_1. The B_2 representation is degenerate with B_1 and, hence, omitted in the calculations. A second set of CI calculations has been done by including spin−orbit interactions in the Hamiltonian. The Λ-S CI energies are kept in the diagonals, whereas the spin−orbit coupling terms occupy the off-diagonal blocks of the Hamiltonian. These off-diagonal elements are obtained from pairs of selected CI wave functions by using spin-projection techniques and the Wigner-Eckart theorem. The sizes of the secular equations for A_1, A_2, and B_1 representations are 44, 45, and 45, respectively. In the present calculations, all 22 Λ-S states, which correlate with the lowest two dissociation limits, are allowed to interact in the spin−orbit CI. Potential energy curves and spectroscopic properties of Ω components are obtained from the resulting eigenvalues and eigenfunctions.

Potential energy curves are numerically fitted into polynomials as a function of the internuclear distance. The nuclear Schrödinger equations are then solved to obtain vibrational energies and wave functions.[49] The dipole transition matrix elements are calculated for the pair of vibrational functions involved in a given transition. Subsequently, Einstein coefficients of spontaneous emission and transition probabilities are computed. The radiative lifetimes of the upper states at the lowest few vibrational levels are also estimated.

III. Results and Discussion

Spectroscopic Properties and Potential Energy Curves of Λ-S States. Experimental atomic spectra of both Ga and Bi atoms were known accurately long ago.[50] The ground-state ($4s^24p;{}^2P_u$) Ga atom combines with the ground-state ($6p^3;{}^4S_u$) Bi to generate four low-lying states such as $^3\Sigma^-$, $^3\Pi$, $^5\Sigma^-$, and $^5\Pi$. The next two excited states of Ga, namely, $4s^25s\ ^2S$ and $4s^25p\ ^2P$, consist of Rydberg functions and are lying nearly 25 000 cm^{-1} above the ground state. On the other hand, the first excited state ($6p^3;{}^2D_u$) Bi atom is low-lying, and it does not have any Rydberg function. Energetically, the next dissociation limit of GaBi correlates with the ground state (^2P_u) of Ga and first excited state (^2D_u) of Bi. There are nine singlets and nine triplets of Σ^+, $\Sigma^-(2)$, $\Pi(3)$, $\Delta(2)$, and Φ symmetries, which converge with the $Ga(^2P_u) + Bi(^2D_u)$ asymptote. The calculated value of the relative energy of this dissociation limit has been found to be lower than the j-averaged experimental value by about 2000 cm^{-1}. The observed spin−orbit splitting between $^2D_{5/2}$ and $^2D_{3/2}$ components of Bi is considerably large.

The computed potential energy curves of triplet and quintet states of GaBi are shown in Figure 1a, whereas the singlet-

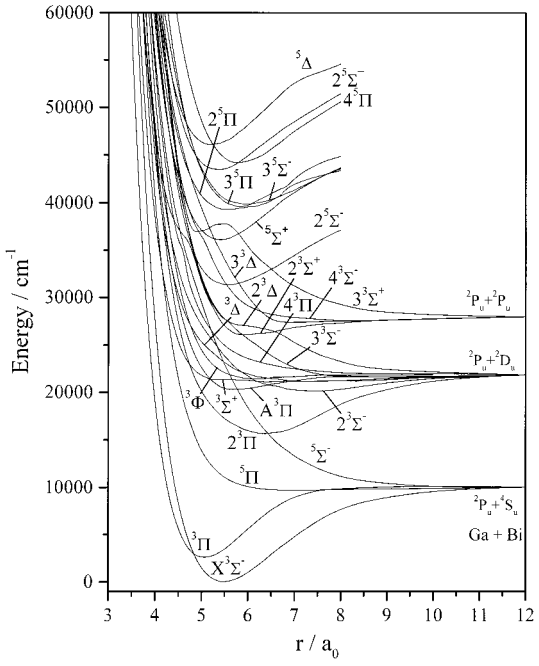

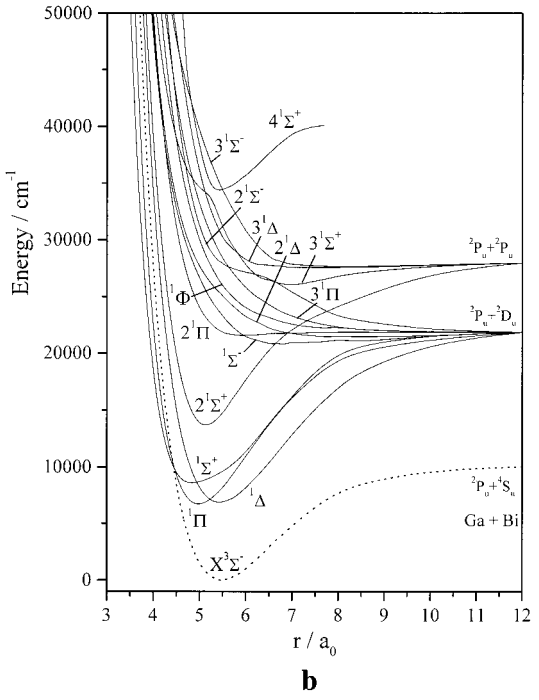

Figure 1. (a) Potential energy curves of triplet and quintet Λ-S states of GaBi. (b) Potential energy curves of singlet Λ-S states of GaBi.

state curves are plotted in Figure 1b. There are 19 bound states within 46 000 cm^{-1} of energy, whereas the remaining states are repulsive in nature. Spectroscopic constants of these Λ-S states are reported in Table 1. Analogous to other group III−V molecules such as GaP, GaAs, GaSb, etc., the ground-state GaBi has a X $^3\Sigma^-$ symmetry, which is represented dominantly by an open shell configuration $...\sigma^2\sigma^{*2}\sigma'^2\pi^2$ ($c^2 = 0.89$). The equilibrium bond length and vibrational frequency of the ground state of GaBi are 2.90 Å and 152 cm^{-1}, respectively. Although no experimental or theoretical data are available even for the ground state of GaBi, our calculated values show the correct trend, when compared with those of the isovalent GaP, GaAs, and GaSb molecules. At r_e, the σ MO is mostly s orbital localized on Bi and a weakly bonding of s(Ga) and s(Bi) atomic orbitals. The next σ^* orbital is antibonding comprising s(Ga) and s, p_z(Bi) atomic orbitals, whereas σ' is somewhat complex in nature. It is found that σ' is strongly bonding of p_z(Ga) and p_z(Bi) but weakly antibonding consisting of s orbitals of Ga and Bi atoms. When SCF MOs are analyzed further in the Franck−Condon region, the first occupied π MO is almost pure $p_{x,y}$(Bi) orbitals, but a very weak bonding characteristic with $p_{x,y}$(Ga) has been noted. The next π^* is, however, strongly antibonding comprising $p_{x,y}$ orbitals of Ga and Bi. The ground-state dissociation energy (D_e) of GaBi, estimated from the Λ-S MRDCI energy at $r = 15.0$ a_0, is found to be 1.24 eV, which is somewhat smaller than the probable value of 1.60 ± 0.17 eV obtained from the mass spectrometric determination.[17] The discrepancy is because of the absence of the correlation of 20 d electrons in the CI step. Moreover, some disagreement will remain because of the effective core potentials used in the calculations.

TABLE 1: Spectroscopic Constants of Low-Lying Λ-S States of GaBi

state	T_e/cm^{-1}	r_e/Å	ω_e/cm^{-1}
$X^3\Sigma^-$	0	2.90	152
$^3\Pi$	2 547	2.68	176
$^1\Pi$	6 668	2.64	194
$^1\Delta$	6 853	2.87	161
$^1\Sigma^+$	8 453	2.58	161
$2^1\Sigma^+$	13 731	2.71	215
$2^3\Pi$	15 676	3.37	92
$A^3\Pi$	20 262	3.02	110
$2^3\Sigma^+$	26 052	3.18	101
$3^1\Sigma^+$	26 074	3.69	77
$2^5\Sigma^-$	31 283	2.96	131
$4^1\Sigma^+$	34 137	2.80	148
$^5\Sigma^+$	36 088	2.86	152
$2^5\Pi$	39 280	2.93	126
$3^5\Pi$	39 409	3.14	134
$3^5\Sigma^-$	39 824	3.15	107
$2^5\Sigma^+$	43 418	2.83	156
$4^5\Pi$	44 123	3.08	144
$^5\Delta$	46 028	2.76	161

The ground-state electronic configuration generates two other singlet Λ-S states, namely, $^1\Delta$ and $2^1\Sigma^+$, which are strongly bound. As seen from Figure 1b, the $^1\Delta$ state correlates with Bi(^2D_u), whereas $2^1\Sigma^+$ dissociates into the second excited state (^2P_u) of the Bi atom. Although the $^1\Delta$ state is pure around r_e, the $2^1\Sigma^+$ state has a contribution of a closed-shell configuration $...\sigma^2\sigma^{*2}\pi^4$ (c^2=0.18) and an excited configuration such as $... \sigma^2\sigma^{*2}\pi^3\pi^*$ (c^2=0.14). The r_e and ω_e values of the $^1\Delta$ state (see Table 1) are found to be quite similar to those of the ground state. The spectroscopic constants of the $2^1\Sigma^+$ state are somewhat different. The potential energy curves of $^1\Sigma^+$ and $2^1\Sigma^+$ in Figure 1b have shown the appearance of a strong avoided crossing around 5.3 a_0. This has been confirmed by analyzing CI wave functions at several bond distances before and after $r = 5.3$ a_0. As a result of this avoided crossing, the fitted adiabatic curve estimates a shorter bond length ($r_e = 2.71$ Å) and longer ω_e (=215 cm^{-1}) for the $2^1\Sigma^+$ state of GaBi.

The first excited state ($^3\Pi$) of GaBi is lying only 2547 cm^{-1} above the ground state. The equilibrium bond length of the $^3\Pi$ state is much shorter than the ground-state bond. The nature of the potential energy curve and spectroscopic constants are analogous to other group III−V molecules. The $^3\Pi$ state originates mainly from the $\sigma \rightarrow \pi^*$ excitation. However, some contribution also comes from another single excitation $\sigma' \rightarrow \pi^*$. The singlet counterpart of $^3\Pi$ originates from the same set of configurations. In the present MRDCI calculations, the splitting between $^3\Pi$ and $^1\Pi$ is estimated to be 4121 cm^{-1}. The

TABLE 2: Composition of Λ-S States of GaBi at r_e

state	configuration (% contributions)
$X^3\Sigma^-$	$\sigma^2\sigma^{*2}\sigma'^2\pi^2$(89)
$^3\Pi$	$\sigma^2\sigma^{*2}\sigma'\pi^3$(73), $\sigma^2\sigma^{*2}\sigma'\pi^2\pi^*$(14)
$^1\Pi$	$\sigma^2\sigma^{*2}\sigma'\pi^3$(73), $\sigma^2\sigma^{*2}\sigma'\pi^2\pi^*$(14), $\sigma^2\sigma^*\sigma'^2\pi^2\pi^*$(1)
$^1\Delta$	$\sigma^2\sigma^{*2}\sigma'^2\pi^2$(87), $\sigma^2\sigma^{*2}\sigma'^2\pi\pi^*$(2)
$^1\Sigma^+$	$\sigma^2\sigma^{*2}\pi^4$(48), $\sigma^2\sigma^{*2}\pi^3\pi^*$(23), $\sigma^2\sigma^{*2}\sigma'^2\pi^2$(12), $\sigma^2\sigma^*\sigma'\pi^4$(3)
$2^1\Sigma^+$	$\sigma^2\sigma^{*2}\sigma'^2\pi^2$(52), $\sigma^2\sigma^{*2}\pi^4$(18), $\sigma^2\sigma^{*2}\pi^3\pi^*$(14), $\sigma^2\sigma^{*2}\sigma'^2\pi\pi^*$(2)
$2^3\Pi$	$\sigma^2\sigma^{*2}\sigma'\pi^2\pi^*$(53), $\sigma^2\sigma^{*2}\sigma'\pi^3$(27), $\sigma^2\sigma^{*2}\sigma_4\pi^2\pi^*$(2), $\sigma^2\sigma^{*2}\sigma_4\pi^3$(2), $\sigma^2\sigma^{*2}\sigma_6\pi^2\pi^*$(2), $\sigma^2\sigma^{*2}\sigma'\pi^2\pi'$(1)
$A^3\Pi$	$\sigma^2\sigma^{*2}\sigma'\pi^2\pi^*$(84), $\sigma^2\sigma^*\sigma'^2\pi^2\pi^*$(3)
$2^3\Sigma^+$	$\sigma^2\sigma^{*2}\sigma'^2\pi\pi^*$(54), $\sigma^2\sigma^{*2}\pi^3\pi^*$(25), $\sigma^2\sigma^{*2}\sigma'\sigma_6\pi\pi^*$(4), $\sigma^2\sigma^{*2}\pi^2\pi^{*2}$(2)
$3^1\Sigma^+$	$\sigma^2\sigma^{*2}\sigma'^2\pi\pi^*$(54), $\sigma^2\sigma^{*2}\sigma'\sigma_4\pi\pi^*$(10), $\sigma^2\sigma^{*2}\sigma'^2\pi^2$(8), $\sigma^2\sigma^{*2}\pi^4$(6), $\sigma^2\sigma^{*2}\pi^3\pi^*$(4)
$2^5\Sigma^-$	$\sigma^2\sigma^{*2}\sigma'\sigma_5\pi^2$(79), $\sigma^2\sigma^{*2}\sigma'\sigma_6\pi^2$(4), $\sigma^2\sigma^{*2}\sigma'\sigma_4\pi^2$(3), $\sigma^2\sigma^{*2}\sigma'\sigma_9\pi^2$(2)
$4^1\Sigma^+$	$\sigma^2\sigma^{*2}\pi^2\pi^{*2}$(30), $\sigma^2\sigma^{*2}\pi^4$(14), $\sigma^2\sigma^{*2}\pi^3\pi^*$(10), $\sigma^2\sigma^*\sigma'\pi^2\pi^{*2}$(9), $\sigma^2\sigma^*\sigma'\pi^3\pi^*$(8), $\sigma^2\sigma^*\sigma'\pi^4$(6), $\sigma^2\sigma^{*2}\sigma'^2\pi\pi^*$(4)
$^5\Sigma^+$	$\sigma^2\sigma^{*2}\pi^2\pi^{*2}$(55), $\sigma^2\sigma^*\sigma'\pi^2\pi^{*2}$(18), $\sigma^2\sigma^*\sigma'\pi^3\pi^*$(13), $\sigma^2\sigma'^2\pi^2\pi^{*2}$(1)
$2^5\Pi$	$\sigma^2\sigma^{*2}\sigma'\pi^2\pi'$(88)
$3^5\Pi$	$\sigma^2\sigma^*\sigma'^2\pi^2\pi^*$(58), $\sigma^2\sigma^{*2}\sigma_6\pi^2\pi^*$(9), $\sigma^2\sigma^{*2}\sigma'\pi\pi^{*2}$(5), $\sigma^2\sigma^{*2}\sigma_4\pi^2\pi^*$(5), $\sigma^2\sigma^*\sigma'^2\pi\pi^{*2}$(3), $\sigma^2\sigma^*\sigma'\sigma_6\pi^2\pi^*$(2), $\sigma^2\sigma^*\sigma'^2\pi^2\pi_5$(2), $\sigma^2\sigma^{*2}\sigma_5\pi^2\pi^*$(1)
$3^5\Sigma^-$	$\sigma^2\sigma^{*2}\sigma'\sigma_4\pi^2$(45), $\sigma^2\sigma^{*2}\sigma'\sigma_6\pi^2$(40), $\sigma^2\sigma^{*2}\sigma'\sigma_{10}\pi^2$(1)
$2^5\Sigma^+$	$\sigma^2\sigma^*\sigma'\pi^3\pi^*$(50), $\sigma^2\sigma^{*2}\pi^2\pi^{*2}$(21), $\sigma^2\sigma^*\sigma'\pi^2\pi^{*2}$(15)
$4^5\Pi$	$\sigma^2\sigma^{*2}\sigma'\pi\pi^{*2}$(53), $\sigma^2\sigma^*\sigma'^2\pi\pi^{*2}$(18), $\sigma^2\sigma^{*2}\sigma_6\pi^2\pi^*$(5), $\sigma^2\sigma^{*2}\sigma_4\pi^2\pi^*$(3), $\sigma^2\sigma^{*2}\sigma_6\pi\pi^{*2}$(3), $\sigma^2\sigma^*\sigma'^2\pi^2\pi^*$(2), $\sigma^2\sigma^*\sigma'\sigma_6\pi^2\pi^*$(1)
$^5\Delta$	$\sigma^2\sigma^*\sigma'\pi^3\pi^*$(80), $\sigma^2\sigma^*\sigma'\pi^2\pi^{*2}$(5), $\sigma^2\sigma^*\sigma'\pi^3\pi_4$(3)

$^1\Pi$ state has even shorter bond length and longer ω_e than $^3\Pi$. The singlet state is much more strongly bound, and it correlates with the excited state (^2D_u) of Bi, whereas $^3\Pi$ dissociates into the ground-state atoms. The greater stability of the Ga−Bi bond in $^{1,3}\Pi$ states is attributed to the increase in the delocalization of the π MO. The fourth excited state is assigned as $^1\Sigma^+$, which has the shortest bond length of all low-lying states of GaBi reported here. The MRDCI-estimated transition energy of the $^1\Sigma^+$ state is 8453 cm^{-1}. Because of the avoided crossing with $2^1\Sigma^+$, three dominant configurations contribute strongly. At the equilibrium bond length, the closed-shell configuration $...\sigma^2\sigma^{*2}\pi^4$ has only 48% contribution to the composition of the $^1\Sigma^+$ state. As seen from Figure 1a, the potential energy curve of the $2^3\Pi$ state has a shallow potential well at a longer bond distance (r_e = 3.37 Å). The vibrational frequency is only 92 cm^{-1}. The existence of this minimum is mainly due to a strong avoided crossing between the curves of $^3\Pi$ and $2^3\Pi$ states. The MRDCI wave functions of the lowest two roots of the $^3B_1$ irreducible representation show that the $2^3\Pi$ state is described predominantly by $...\sigma^2\sigma^{*2}\sigma'\pi^3$ in the bond length region above 7.0 a_0, whereas in the shorter bond length region, it is composed of $...\sigma^2\sigma^{*2}\sigma'\pi^2\pi^*$. The appearance of such a broad potential minimum of the $2^3\Pi$ state is a general feature for all group III−V diatomic molecules. Earlier MRDCI calculations on isovalent molecules of group III and IV have revealed identical characteristics of the potential curves of the $2^3\Pi$ state. The $2^3\Pi-X\ ^3\Sigma^-$ transition is always expected to be very weak because of the longer r_e of the upper state.

There exists four $^3\Pi$ states, which originate from the $...\sigma^2\sigma^{*2}\sigma'\pi^2\pi^*$ configuration. Besides $2^3\Pi$, the $3^3\Pi$ state is bound and spectroscopically important, whereas the remaining $4^3\Pi$ and $5^3\Pi$ states are repulsive in nature. We shall, therefore, focus our attention on the $3^3\Pi$ state only. Keeping an analogy with the observed $A^3\Pi$ state of GaAs, we have designated $3^3\Pi$ as the A state. For GaBi, the $A^3\Pi$ state is weakly bound with the calculated binding energy of about 1700 cm^{-1} only. The computed r_e and ω_e of the $A^3\Pi$ state of GaBi are 3.02 Å and 110 cm^{-1}, respectively. The $A^3\Pi-X^3\Sigma^-$ band of GaBi is expected to be around 20 262 cm^{-1}. Previous MRDCI calculations on GaX (X = P, As, Sb) at the same level have shown that the transition energies of the $A^3\Pi$ state follow the expected trend as T_e(GaP) > T_e(GaAs) > T_e(GaSb) > T_e(GaBi). In the Franck−Condon region of the potential energy curve, the $A^3\Pi$ state remains pure with 84% contribution of the dominant configuration (see Table 2). Because GaBi is comparatively heavy, the spin−orbit effect on the $A^3\Pi$ state plays a significant role. Figure 1a shows a shallow minimum of the $2^3\Sigma^-$ state, which is bound only by 800 cm^{-1}. Spectroscopically, the $2^3\Sigma^-$ state does not have much significance as the transition to the ground state would be very weak.

The $...\sigma^2\sigma^{*2}\sigma'\pi^2\pi^*$ configuration generates 10 Λ-S states, of which four $^3\Pi$ states are already discussed. Out of three $^1\Pi$ states, $2^1\Pi$ and $3^1\Pi$ dissociate into Ga(^3P_u) + Bi(^2D_u). The present calculations show that the $2^1\Pi$ state is very weakly bound (binding energy ~300 cm^{-1}), whereas $3^1\Pi$ is repulsive. The remaining three states, which originate from the $...\sigma^2\sigma^{*2}\sigma'\pi^2\pi^*$ configuration, are $^{1,3}\Phi$ and $^5\Pi$. Potential energy curves of all three states are repulsive as shown in Figure 1 parts a and b. The $^5\Pi$ state is very low-lying, and it correlates with the lowest dissociation limit.

Unlike other GaX (X = P, As, Sb) molecules, the $^3\Sigma^+$ state of GaBi is very weakly bound. The potential energy curve of this state shows a shallow minimum (see Figure 1a). The computed binding energy of the $^3\Sigma^+$ state is only 750 cm^{-1}. The $2^3\Sigma^+$ state is lying 26 052 cm^{-1} above the ground state with r_e = 3.18 Å and ω_e = 101 cm^{-1}. The compositions of CI wave functions of $^3\Sigma^+$ and $2^3\Sigma^+$ reveal that the appearance of the long-distant minimum in the $2^3\Sigma^+$ state curve is due to an avoided crossing. Two important configurations, namely, $\sigma^2\sigma^{*2}\pi^3\pi^*$ and $\sigma^2\sigma^{*2}\sigma'^2\pi\pi^*$, mix up strongly in the bond length region above 6.0 a_0. At the potential minimum, the $2^3\Sigma^+$ state is represented by these two configurations as shown in Table 2.

The potential energy curves of $3^1\Sigma^+$ and $4^1\Sigma^+$ states demonstrate an avoided crossing near r = 5.5 a_0, and a broad minimum appears at 3.69 Å. The $3^1\Sigma^+$ state at the long-distant minimum is characterized mainly by $...\sigma^2\sigma^{*2}\sigma'^2\pi\pi^*$. When the diabatic curve is fitted, the estimated r_e and ω_e of the $4^1\Sigma^+$ state are approximately 2.80 Å and 148 cm^{-1}, respectively. The minimum is located at a very high energy with T_e ~ 34 137 cm^{-1}. There exists no other strongly bound singlet states at least up to 45 000 cm^{-1} of energy.

A set of high-lying strongly bound quintet state-curves is noted in Figure 1a. All of these quintets dissociate into higher asymptotes. Only the Franck−Condon region of the curves of these high-lying quintets are shown in Figure 1a. The $2^5\Sigma^-$ state is stable at 2.96 Å with T_e = 31 283 cm^{-1} and ω_e = 131 cm^{-1}. As seen in Table 2, the state is represented by the $...\sigma^2\sigma^{*2}\sigma'\sigma_5\pi^2$ configuration, in which the σ_5 MO has some Rydberg character of 7s atomic orbital of Bi. Because we have not used any

TABLE 3: Dissociation Relation between Ω States and Atomic States of GaBi

Ω state	atomic states Ga + Bi	relative energy/cm^{-1} expt.[a]	calc.
0^+, 0^-, 1(2), 2	$^2P_{1/2} + {}^4S_{3/2}$	0	0
$0^+(2)$, $0^-(2)$, 1(3), 2(2), 3	$^2P_{3/2} + {}^4S_{3/2}$	826	860
0^+, 0^-, 1(2), 2	$^2P_{1/2} + {}^2D_{3/2}$	11419	12185
$0^+(2)$, $0^-(2)$, 1(3), 2(2), 3	$^2P_{3/2} + {}^2D_{3/2}$	12245	13215
0^+, 0^-, 1(2), 2(2), 3	$^2P_{1/2} + {}^2D_{5/2}$	15438	16981
$0^+(2)$, $0^-(2)$, 1(4), 2(3), 3(2), 4	$^2P_{3/2} + {}^2D_{5/2}$	16264	17932

[a] Reference 50.

additional Rydberg function in the basis set, the spectroscopic properties of this state, obtained in our calculations, may not be very accurate. Both $^5\Sigma^+$ and $2^5\Sigma^+$ states are found to be strongly bound. These two states have similar r_e and ω_e values with an energy separation of about 7330 cm^{-1}. Three configurations such as $...\sigma^2\sigma^{*2}\pi^2\pi^{*2}$, $...\sigma^2\sigma^*\sigma'\pi^3\pi^*$, and $...\sigma^2\sigma^*\sigma'\pi^2\pi^{*2}$ contribute strongly in the description of both $^5\Sigma^+$ and $2^5\Sigma^+$ states. Table 2 shows the actual contribution of each configuration, which does not contain any Rydberg type orbital. There are three closely spaced $^5\Pi$ states, which are strongly bound and dissociate into higher limits. An avoided crossing between the potential curves of $2^5\Pi$ and $3^5\Pi$ states is also noted. The $2^5\Pi$ state with $T_e = 39\ 280$ cm^{-1} is composed of a dominant configuration $...\sigma^2\sigma^{*2}\sigma'\pi^2\pi'$ ($c^2 = 0.8$), where the π MO is the nonbonding $p_{x,y}$(Bi) atomic orbitals and π' is a bonding combination of $p_{x,y}$ atomic orbitals of Ga and Bi. The $3^5\Pi$ state is described by many configurations of which $...\sigma^2\sigma^*\sigma'^2\pi^2\pi^*$ is the dominant one. The estimated transition energy of the $4^5\Pi$ state is 44 123 cm^{-1}, while r_e and ω_e are 3.08 Å and 144 cm^{-1}, respectively. The configuration, which dominates the $4^5\Pi$ state, arises from a double excitation $...\sigma'^2\pi^2 \rightarrow ...\sigma'\pi\pi^{*2}$. Other excited configurations also contribute to a small extent to the characterization of this state. The remaining two quintet states, namely, $3^5\Sigma^-$ and $^5\Delta$, are also found to be strongly bound. The $3^5\Sigma^-$ state is lying very close to $2^5\Pi$ and $3^5\Pi$, whereas the transition energy of the $^5\Delta$ state is estimated to be 46 028 cm^{-1}. The Ga−Bi bond in the $^5\Delta$ state is unusually short with $r_e = 2.76$ Å. The MRDCI wave functions show that the dominant configuration for the description of the $^5\Delta$ state is $...\sigma^2\sigma^*\sigma'\pi^3\pi^*$ ($c^2 = 0.8$). Some spin-forbidden transitions from the spin components of these quintets are expected to take place.

Low-Lying Ω States and Their Spectroscopic Properties. Effects of the spin−orbit coupling on the spectroscopic properties of the GaBi molecule will be discussed in this section. The spin−orbit interaction is introduced by the inclusion of the spin−orbit operators derived from RECP.[39,40] All 22 Λ-S states, which correlate with the lowest two dissociation limits, are allowed to interact through the spin−orbit coupling. The lowest two limits split into six asymptotes. Table 3 displays relative energies of the dissociated atoms with which Ω states correlate. The computed energies are found to be overestimated as compared with the observed data. The experimental spin−orbit splitting for the ^2P state of Ga agrees well with the value of the splitting obtained from the MRDCI calculations at $r = 15$ a_0. The computed ($^2D_{5/2}-{}^2D_{3/2}$) separation for the Bi atom is found to be around 4700 cm^{-1}, whereas the experimental splitting[50] is 4019 cm^{-1}. The discrepancies are, therefore, within the limit of accuracy for the RECP-based MRDCI calculations. Relative energies of the four limits of Ga(^2P_u) + Bi(^2D_u) are calculated to be higher than the observed values by 750−1700 cm^{-1}. However, at the same level of MRDCI calculations, energies of the dissociation limits for GaBi show considerably smaller discrepancies than those for GaP, GaAs, and GaSb.

TABLE 4: Spectroscopic Constants of Low-Lying Ω States of GaBi

state	T_e/cm^{-1}	r_e/Å	ω_e/cm^{-1}
$X^3\Sigma^-_{0^+}$	0	2.90	133
$X^3\Sigma^-_1$	463	2.81	149
$^3\Pi_2$	1332	2.73	164
$^3\Pi_{0^+}$	5147	2.75	163
$^3\Pi_1$	9156	2.83	137
$^3\Pi_{0^-}$	10061	2.77	117
2(III)	13790	2.87	167
0^+(IV)	15283	2.75	200
0^-(III)	15921	3.01	136
0^+(V)	20368	3.24	78
A $^3\Pi_{0^+}$	25200	3.27	71

Figure 2 parts a−d show the calculated potential energy curves of a few low-lying Ω states of 0^+, 0^-, 1, 2, 3, and 4 symmetries. There are 51 Ω states arising out of 22 Λ-S states interacted in the spin−orbit coupling. Spectroscopic parameters of 11 bound Ω states are reported in Table 4. Two spin−orbit components of the ground state of GaBi are separated by 463 cm^{-1}. The $X^3\Sigma^-_{0^+}$ state is found to be lower in energy than the other component. The zero field splittings [$^3\Sigma^-(1X_2)-{}^3\Sigma^-(0^+X_1)$] of the isovalent lighter molecules such as GaP, GaAs, and GaSb are much smaller than that of GaBi. The r_e and ω_e values of the two components of $X^3\Sigma^-$, obtained by fitting their adiabatic curves, differ considerably because of their different magnitudes of the spin−orbit matrix elements. Table 5 demonstrates the compositions of bound Ω states in their adiabatic curves at four representative bond distances. In the Franck−Condon region, $X^3\Sigma^-_{0^+}$ is composed of two strongly interacting components such as $X^3\Sigma^-_{0^+}$ and $^1\Sigma^+_{0^+}$, whereas for the $X^3\Sigma^-_1$ state, the mixings of $X^3\Sigma^-_1$ with $^3\Pi_1$ and $^1\Pi_1$ are also found to be sufficiently large. As a result, the equilibrium bond length of $X^3\Sigma^-_1$ becomes shorter and ω_e larger than the $X^3\Sigma^-_{0^+}$ counterpart. At the shorter bond distance region (say, $r = 4.5$ a_0) of the adiabatic potential curve of $X\ ^3\Sigma^-_1$, the $^3\Pi_1$ component dominates, but $X^3\Sigma^-_1$ and $^1\Pi_1$ components also contribute strongly.

The spin components of $^3\Pi$ split as 2, 0^+, 1, and 0^- in the increasing order of energy. As expected, the magnitude of the spin−orbit coupling is considerably large. Although none of these states remains as pure $^3\Pi$, we have designated 2, 0^+(II), 1, and 0^- as components of $^3\Pi$. The largest splitting between $^3\Pi_2$ and $^3\Pi_{0^-}$ components is computed to be 8729 cm^{-1}. Many avoided crossings exist in the potential energy curves of these components. Throughout the curve of the lowest $\Omega = 2$ state, the dominant $^3\Pi_2$ component interacts strongly with $^1\Delta_2$. However, other components such as $^5\Sigma^-_2$, $2^3\Pi_2$, and $^5\Pi_2$ begin to couple with $^3\Pi_2$ at longer bond distances. Spectroscopic constants of all four components of $^3\Pi$ are estimated by fitting the adiabatic curves. The $^3\Pi_{0^+}$ state is located at 5147 cm^{-1} with $r_e = 2.75$ Å and $\omega_e = 163$ cm^{-1}. At r_e, this state is dominated by $^3\Pi$, but the mixings with $2^1\Sigma^+_{0^+}$(31%) and $X^3\Sigma^-_{0^+}$(5%) components are considerably large. As seen from Table 5, the contribution of $^3\Pi_{0^+}$ decreases, whereas the $X^3\Sigma^-_{0^+}$ component begins to dominate in the shorter bond-length region. The second $\Omega = 1$ state is described predominantly by the $^3\Pi_1$ component, but a strong coupling with $X^3\Sigma^-_1$ shifts the equilibrium bond length to the longer value ($r_e = 2.83$ Å) and ω_e to a larger value of 137 cm^{-1}. The $^3\Pi_1$ state is shifted up by a large extent because of the strong coupling. The transition energy of the $^3\Pi_1$ state, estimated from the adiabatic curve, is found to be 9156 cm^{-1}. The lowest root of $\Omega = 0^-$ symmetry is seen to have a very shallow minimum around 2.77 Å, and it holds only two vibrational energy levels.

TABLE 5: Compositions of Ω States of GaBi at Four Representative Bond Lengths

	composition (in percentage contribution)			
state	$r = 4.5a_0$	$r = 5.0a_0$	$r = r_e$	$r = 7.0a_0$
$X^3\Sigma^-_{0^+}$	$^3\Pi(41)$,X $^3\Sigma^-(28)$, $^1\Sigma^+(25)$,$^5\Pi(2)$	$X^3\Sigma^-(65)$, $^1\Sigma^+(13)$, $^3\Pi(7)$,$^5\Pi(3)$	$X^3\Sigma^-(73)$,$^3\Pi(6)$, $^1\Sigma^+(14)$,$^5\Pi(3)$	$X^3\Sigma^-(72)$, $^1\Sigma^+(13)$, $^5\Pi(4)$,2 $^1\Sigma^+(2)$,$6^3\Pi(3)$
$X^3\Sigma^-_1$	$^3\Pi(46)$,X $^3\Sigma^-(27)$, $^1\Pi(22)$	$X^3\Sigma^-(43)$,$^3\Pi(34)$, $^1\Pi(17)$	$X^3\Sigma^-(50)$,$^3\Pi(28)$, $^1\Pi(14)$	$X^3\Sigma^-(60)$, $^3\Pi(12)$,$^1\Pi(8)$, $2^3\Pi(4)$,$^5\Pi(4)$, $^5\Sigma^-(1)$
$^3\Pi_2$	$^3\Pi(86)$,$^1\Delta(10)$	$^3\Pi(79)$,$^1\Delta(15)$	$^3\Pi(77)$,$^1\Delta(17)$	$^3\Pi(55)$, $^1\Delta(14)$, $^5\Sigma^-(9)$, $2^3\Pi(6)$,$3^1\Delta(4)$,$^5\Pi(3)$
$^3\Pi_{0^+}$	$X^3\Sigma^-(47)$, $2^1\Sigma^+(28)$,$^3\Pi(16)$	$^3\Pi(52)$,2 $^1\Sigma^+(32)$, $X^3\Sigma^-(9)$	$^3\Pi(58)$,2 $^1\Sigma^+(31)$, $X^3\Sigma^-(5)$	$^3\Pi(69)$,2 $^1\Sigma^+(9)$,3 $^1\Sigma^+(8)$, $4^3\Pi(4)$,$5^3\Pi(4)$
$^3\Pi_1$	$^3\Pi(48)$,X $^3\Sigma^-(40)$, $^1\Pi(8)$	$^3\Pi(51)$,X $^3\Sigma^-(44)$, $^5\Pi(1)$	$^3\Pi(55)$,X $^3\Sigma^-(39)$, $^1\Pi(2)$,$^5\Pi(2)$	$^5\Pi(62)$,2 $^3\Sigma^+(11)$,4 $^3\Sigma^-(5)$, 3 $^3\Sigma^-(2)$,$4^3\Pi(2)$,$5^3\Pi(2)$
$^3\Pi_{0^-}$	$^3\Pi(96)$, $^3\Sigma^+(1)$	$^3\Pi(95)$,2 $^1\Sigma^-(1)$	$^3\Pi(90)$,$2^3\Pi(4)$, $2^1\Sigma^-(3)$	$^5\Pi(62)$, $^3\Pi(7)$,$5^3\Pi(6)$, 2 $^3\Sigma^+(6)$,$A^3\Pi(3)$,2 $^1\Sigma^-(3)$
2(III)	$^5\Pi(64)$,$^3\Delta(10)$, $2^1\Delta(6)$,$2^3\Delta(5)$, $5^3\Pi(4)$,$A^3\Pi(3)$	$^5\Pi(61)$,$2^3\Delta(10)$, $^1\Delta(5)$,$2^1\Delta(4)$, $^3\Pi(4)$,$5^3\Pi(4)$	$^1\Delta(76)$, $^3\Pi(18)$, $2^3\Delta(2)$	$^5\Sigma^-(29)$,$2^3\Pi(24)$,$^3\Pi(11)$, $3^1\Delta(8)$,$6^3\Pi(7)$,$5^3\Pi(4)$, $^1\Delta(3)$,$^5\Pi(3)$,$4^3\Pi(2)$
0^+(IV)	$^5\Pi(70)$, $2^3\Pi(12)$, $5^3\Pi(8)$,X $^3\Sigma^-(3)$	$^1\Sigma^+(46)$,$^5\Pi(40)$, $2^3\Pi(5)$	$^1\Sigma^+(69)$,$^5\Pi(19)$, $^3\Pi(3)$,X $^3\Sigma^-(3)$	$^1\Sigma^+(40)$,$2^3\Pi(39)$, X $^3\Sigma^-(8)$,$4^3\Pi(5)$
0^-(III)	$2^3\Pi(40)$, $^3\Sigma^+(39)$, $^1\Sigma^-(7)$,$A^3\Pi(5)$, $2^1\Sigma^-(4)$,$^5\Pi(3)$	$2^3\Pi(52)$, $^3\Sigma^+(24)$, $2^1\Sigma^-(10)$,$^5\Pi(6)$, $^1\Sigma^-(2)$,2 $^3\Sigma^+(2)$	$2^3\Pi(50)$,$^3\Pi(16)$, $^3\Sigma^+(12)$,2 $^1\Sigma^-(10)$, $2^3\Sigma^+(5)$	$^5\Sigma^-(78)$,3 $^3\Sigma^+(11)$,$6^3\Pi(8)$
0^+(V)	$2^3\Pi(38)$,2 $^1\Sigma^+(30)$, $A^3\Pi(10)$,$^5\Pi(9)$, $^3\Pi(6)$,X $^3\Sigma^-(5)$	$2^3\Pi(55)$,$^5\Pi(20)$, $A^3\Pi(11)$,2 $^1\Sigma^+(7)$, $5^3\Pi(2)$,2 $^3\Sigma^-(2)$	$2^3\Pi(41)$, $^5\Pi(23)$, $A^3\Pi(13)$, 2 $^1\Sigma^+(8)$, $3^1\Sigma^+(6)$,2 $^3\Sigma^-(5)$	$^5\Pi(25)$,$A^3\Pi(19)$, $2^3\Pi(12)$, $2^1\Sigma^+(12)$,2 $^3\Sigma^-(10)$, $^1\Sigma^+(9)$,3 $^1\Sigma^+(5)$
$A^3\Pi_{0^+}$	$A^3\Pi(79)$,$2^3\Pi(7)$, $3^1\Sigma^+(6)$,2 $^1\Sigma^+(3)$, $5^3\Pi(3)$	$A^3\Pi(76)$,$2^3\Pi(17)$	$A^3\Pi(52)$,2 $^3\Sigma^-(12)$, $3^1\Sigma^+(7)$, $^1\Sigma^+(6)$, $^3\Pi(5)$,$4^3\Pi(4)$	$A^3\Pi(55)$,2 $^3\Sigma^-(20)$, $^1\Sigma^+(9)$,$2^3\Pi(6)$,4 $^3\Sigma^-(3)$

At r_e, the state is almost pure $^3\Pi$ (90%), whereas the state changes its character to the dominant $^5\Pi_{0^-}$ component in the longer bond length region because of the avoided crossing (see Figure 2b). However, we have designated this lowest $\Omega = 0^-$ state as $^3\Pi_{0^-}$. Spectroscopic constants (r_e, ω_e, and T_e) of the $^3\Pi_{0^-}$ state are also obtained by fitting the adiabatic potential curve. The calculations show that the spin−orbit coupling is so strong that the $^3\Pi_{0^-}$ component is pushed up by 7514 cm^{-1}, and the computed transition energy of $^3\Pi_{0^-}$ is 10 061 cm^{-1}.

The potential energy curve of the third $\Omega = 2$ state, which is designated as 2(III), shows a couple of strong avoided crossings in Figure 2c. In the present calculations, the adiabatic curve has been fitted, and the estimated spectroscopic parameters of 2(III) are displayed in Table 4. The 2(III) state at $r_e = 2.87$ Å is mostly the pure component of $^1\Delta$, whereas at the shorter bond distances, the presence of $^5\Pi_2$ dominates (see Table 5). In the longer bond length region, $\Omega = 2$ components of other states such as $^5\Sigma^-$, $^3\Pi$, $2^3\Pi$, etc. contribute strongly. The largest contribution of the $^5\Sigma^-_2$ component to the 2(III) state at $r = 7.0$ a$_0$ is 29%. The only spin−orbit component of a strongly bound $^1\Pi$ state undergoes predissociation. Figure 2d has shown avoided crossings in the potential curve of the third root of $\Omega = 1$. In the shorter bond length region of this curve, the state is dominated by the $^1\Pi_1$ component. Instead of forming a potential minimum, the 1(III) curve quickly falls through a dissociative channel, which is dominated by the repulsive $^5\Pi$ state. An avoided crossing between the curves of third and fourth root of $\Omega = 0^+$ around 5.0 a$_0$ has been noted in Figure 2a. We have fitted the adiabatic curve of the fourth root of 0^+, which is designated as 0^+(IV). Analyzing the wave function, it is found that $^5\Pi_{0^+}$ and $^1\Sigma^+_{0^+}$ components undergo avoided crossing as illustrated in Table 5. At 5.0 a$_0$ of the adiabatic curve, the 0^+(IV) state is composed of almost two equally important states such as $^1\Sigma^+$ and $^5\Pi$, whereas in the shorter bond length region, the state is represented by the dominant $^5\Pi$ state. The equilibrium bond length of the adiabatic 0^+(IV) state is estimated to be 2.75 Å, and the fitted ω_e is found to be somewhat larger because of the avoided crossing.

As a result of the strong spin−orbit coupling, all four components of $2^3\Pi$ change their characteristics to a large extent. In the adiabatic curve of the third root of $\Omega = 0^-$, a minimum has been located at 3.01 Å with $\omega_e = 136$ cm^{-1}. The potential minimum of the adiabatic 0^-(III) curve holds six vibrational nodes. Above 6.2 a$_0$, the 0^-(III) state dissociates through a channel, which is dominated by the repulsive $^5\Sigma^-$ state. Table 5 shows how the compositions of the adiabatic 0^-(III) curve change at different bond distances. As seen in Figure 2a, the fifth root of $\Omega = 0^+$ is weakly bound and is designated as 0^+(V). The minimum of 0^+(V) is lying 20 368 cm^{-1} above the ground state at $r_e = 3.24$ Å. In the Franck−Condon region, the 0^+(V) state is found to be dominated by the 2 $^3\Pi_{0^+}$ component. However, the contributions of other components such as $^5\Pi_{0^+}$, $2^1\Sigma^+_{0^+}$, $A^3\Pi_{0^+}$, $2^3\Pi_{0^+}$, etc. are significant as demonstrated in Table 5.

The $A^3\Pi$ states of all group III−V diatomic molecules draw a special attention. In general, three components with $\Omega = 2$, 1, and 0^- interact strongly with those of the repulsive $^5\Sigma^-$ state. For GaBi, the spin−orbit coupling is so strong that the $A^3\Pi_{2,1,0^-}$ components mix up strongly, and there are no bound states with $\Omega = 1$ and 0^-, which are dominated by $A^3\Pi$. Like other group III−V diatomic molecules, the $A^3\Pi_{0^+}$ component, which is the seventh root of the 0^+ symmetry, is bound. The spectroscopic constants estimated from the adiabatic curve of $A^3\Pi_{0^+}$ are shown in Table 4. The compositions of the $A^3\Pi_{0^+}$ state at four representative bond distances show that the contribution of $A^3\Pi$ is always more than 50%. Therefore, the $A^3\Pi_{0^+}$ component should survive any predissociation, but the state is bound only by 600 cm^{-1}. The dipole allowed transitions from $A^3\Pi_{0^+}$ to the lowest two components $X^3\Sigma^-_{0^+}$ and $X^3\Sigma^-_1$ are also the subject of this study.

Transition Dipole Moments and Radiative Lifetimes of Excited Electronic States. The MRDCI calculations predict several dipole allowed transitions for GaBi. Experimentally or theoretically, no transition has been reported so far. At the Λ-S level, two transitions from $A^3\Pi$, and another two from $2^1\Sigma^+$,

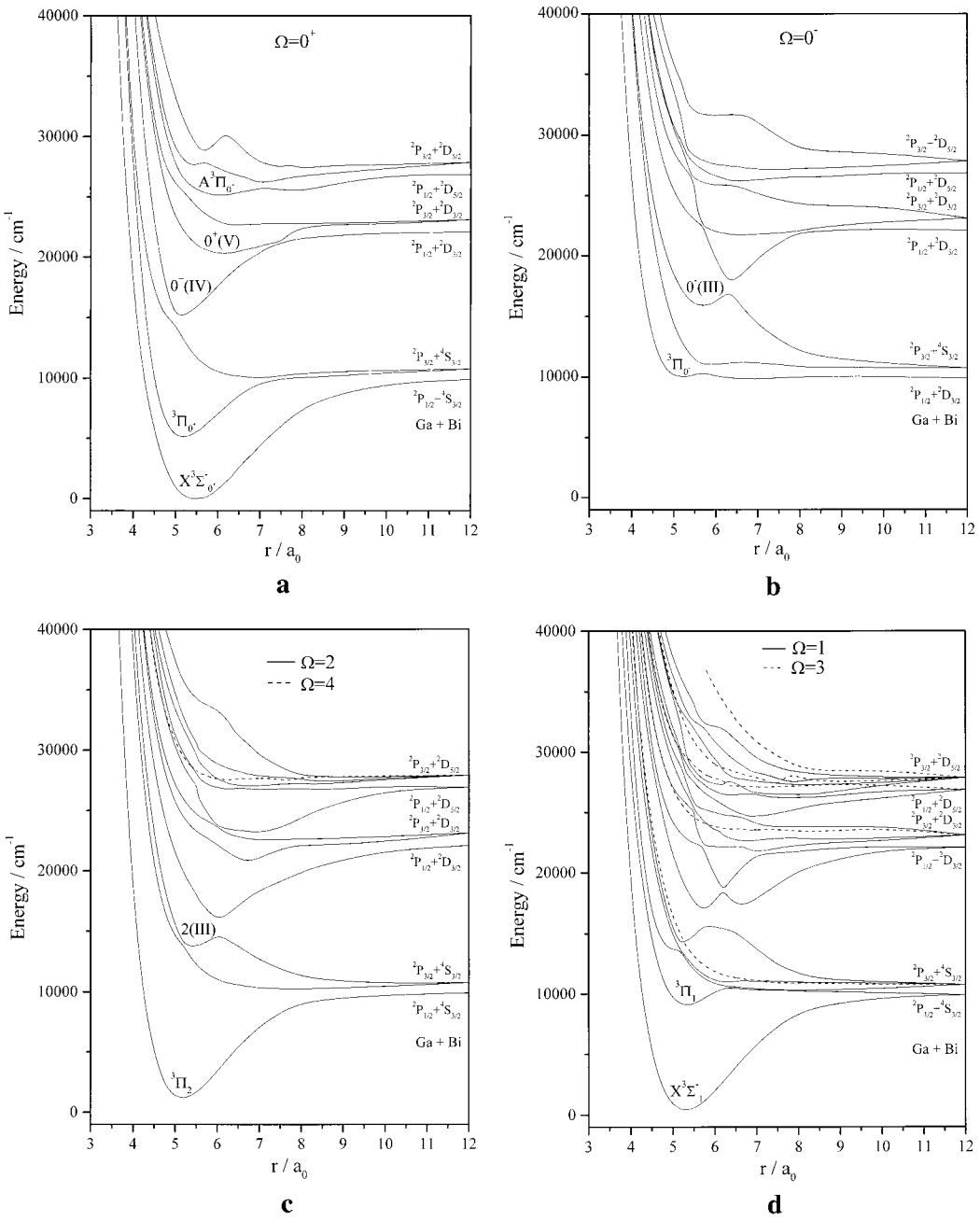

Figure 2. (a) Potential energy curves of the low-lying $\Omega = 0^+$ states of GaBi. (b) Potential energy curves of the low-lying $\Omega = 0^-$ states of GaBi. (c) Potential energy curves of the low-lying $\Omega = 2$ and 4 states of GaBi. (d) Potential energy curves of the low-lying $\Omega = 1$ and 3 states of GaBi.

are possible to take place. The calculated transition moments of these transitions such as $A^3\Pi$-$X^3\Sigma^-$, $A^3\Pi-{}^3\Pi$, $2^1\Sigma^+-{}^1\Pi$, and $2^1\Sigma^+-{}^1\Sigma^+$ are plotted in Figure 3a as a function of the Ga−Bi bond distance. The computed partial lifetimes of the upper states, namely, $A^3\Pi$ and $2^1\Sigma^+$, at three lowest vibrational levels are reported in Table 6. The transition-moment curve for the A−X transition shows a maximum. Although the transition moments of $2^1\Sigma^+-{}^1\Pi$ are higher throughout the curve, the $A^3\Pi-X^3\Sigma^-$ transition is found to be strongest of all. In the Franck−Condon region, transition moments of the $A^3\Pi-{}^3\Pi$ transition are computed to be small and the transition becomes weak. The partial lifetime of $A^3\Pi$ is computed to be 6.2 ms at $v' = 0$. Adding transition probabilities of $A^3\Pi-X^3\Sigma^-$ and $A^3\Pi-{}^3\Pi$ transitions, the total radiative lifetime of $A^3\Pi$ is estimated to be 2.06 μs at the lowest vibrational level. The $2^1\Sigma^+-{}^1\Pi$ transition is considerably strong, and the partial lifetime of the $2^1\Sigma^+$ state at $v' = 0$ is 9.16 μs. On the other hand, the transition such as $2^1\Sigma^+-{}^1\Sigma^+$ is comparatively weak. The computed total lifetime of the $2^1\Sigma^+$ state at $v' = 0$ is found to be 7.6 μs.

The strong spin−orbit coupling changes the nature of the potential energy curves considerably. The $A^3\Pi_{0^+}$ component has been found to be an important state from which many transitions to the stable lower states with $\Delta\Lambda = 0, \pm 1$ are made possible. Figure 3b shows the transition moments of four transitions from the $A^3\Pi_{0^+}$ component as a function of the internuclear distance. The transition probability of the $A\ {}^3\Pi_{0^+}-X^3\Sigma^-_{0^+}$ transition is found to be larger than that of $A\ {}^3\Pi_{0^+}-X^3\Sigma^-_1$. The $A^3\Pi_{0^+}-{}^3\Pi_{0^+}$ transition is considerably strong, and the partial lifetime of the upper state at $v' = 0$ is about 0.83 μs. The transition is, therefore, expected to be observed in the region of 20 000 cm^{-1}. The $A^3\Pi_{0^+}-{}^3\Pi_1$ transition is predicted to be very weak because of the negligible Franck−Condon overlap

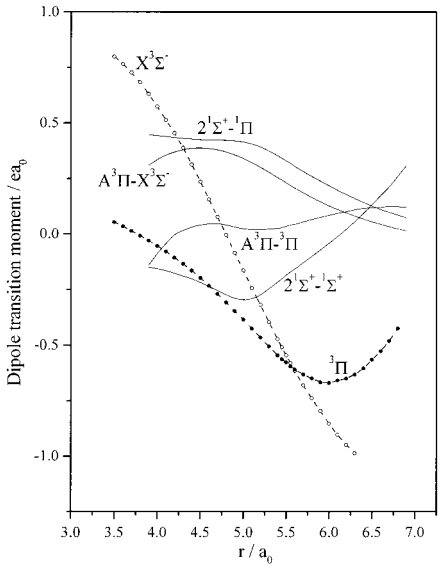

a

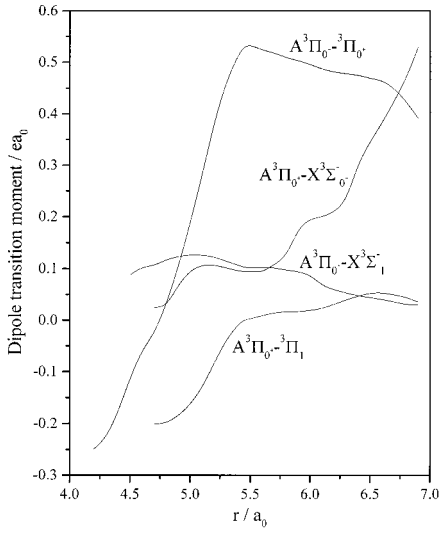

b

Figure 3. (a) Transition-moment functions of four transitions involving Λ-S states, and dipole moment functions of $X^3\Sigma^-$ (dashed open circle) and $^3\Pi$ states (dashed filled circle) of GaBi. (b) Transition-moment functions of transitions from the A $^3\Pi_{0^+}$ component of GaBi.

TABLE 6: Radiative Lifetimes(s) of Some Excited States at Few Lowest Vibrational Levels of GaBi[a]

transition	lifetime of the upper state $v'=0$	$v'=1$	$v'=2$	total lifetime of the upper state at $v'=0$
$A^3\Pi \rightarrow X^3\Sigma^-$	2.06(−6)	2.11(−6)	2.16(−6)	
$A^3\Pi \rightarrow {}^3\Pi$	6.20(−3)	1.60(−3)	8.31(−4)	$\tau(A^3\Pi)$=2.06(−6)
$2\ ^1\Sigma^+ \rightarrow {}^1\Pi$	9.16(−6)	9.18(−6)	9.21(−6)	
$2\ ^1\Sigma^+ \rightarrow {}^1\Sigma^+$	4.59(−5)	4.61(−5)	4.63(−5)	$\tau(2\ ^1\Sigma^+)$=7.6(−6)
$A^3\Pi_{0^+} \rightarrow X^3\Sigma^-_{0^+}$	0.98(−6)	0.89(−6)	0.71(−6)	
$A^3\Pi_{0^+} \rightarrow X^3\Sigma^-_1$	6.33(−6)	6.83(−6)	7.01(−6)	
$A^3\Pi_{0^+} \rightarrow {}^3\Pi_{0^+}$	0.83(−6)	0.70(−6)	0.84(−6)	$\tau(A\ ^3\Pi_{0^+})$=0.42(−6)

[a] Values in parentheses are the powers to the base 10.

term, which is due to the smaller r_e of $^3\Pi_1$ as compared with the r_e of $A^3\Pi_{0^+}$. On the other hand, the potential curve of the $^3\Pi_{0^+}$ component is more strongly bound with many vibrational levels, and it makes the $A^3\Pi_{0^+}-{}^3\Pi_{0^+}$ transition reasonably strong. The estimated total radiative lifetime of the $A^3\Pi_{0^+}$ state, which survives the predissociation, is about 0.42 μs. In Table 7, we have provided the data for the oscillator strengths ($f_{v'v''}$)

TABLE 7: Computed Oscillator Strengths ($f_{v'v''}$) for Transitions from $A^3\Pi_{0^+}(v'')$ to $X^3\Sigma^-_{0^+}$ and $X^3\Sigma^-_1(v')$ Components of GaBi[a]

transition	v″	$v'=0$	$v'=1$	$v'=2$
$A^3\Pi_{0^+}-X^3\Sigma^-_{0^+}$	0	0.1608(−5)	0.7793(−5)	0.2106(−4)
	1	0.1023(−4)	0.3672(−4)	0.6965(−4)
	2	0.3567(−4)	0.9064(−4)	0.1085(−3)
$A^3\Pi_{0^+}-X^3\Sigma^-_1$	0	0.1464(−7)	0.1068(−6)	0.4379(−6)
	1	0.1499(−6)	0.9518(−6)	0.3363(−5)
	2	0.7668(−6)	0.4175(−5)	0.1247(−4)

[a] Values in parentheses are the powers to the base 10.

TABLE 8: Comparison of Spectroscopic Properties of GaX (X = P, As, Sb, Bi) Molecules at the Same Level of MRDCI Calculations

property[a]	GaP[b]	GaAs[c]	GaSb[d]	GaBi
$r_e(X^3\Sigma^-)$, Å	2.50	2.67	2.82	2.90
$\omega_e(X^3\Sigma^-)$, cm^{-1}	268	236	203	176
$D_e(X^3\Sigma^-)$, eV	1.69	1.30	1.30	1.24
$\mu_e(X^3\Sigma^-)$, D	1.86	2.27	2.22	1.29
$T_e(^3\Pi)$, cm^{-1}	782	1066	1573	2547
$r_e(^3\Pi)$, Å	2.26	2.40	2.57	2.68
$\Delta E(^1\Pi - {}^3\Pi)$, cm^{-1}	4725	4875	4394	4121
$T_e(A^3\Pi)$, cm^{-1}	24 145	22 250	21 508	20 262
$r_e(A^3\Pi)$, Å	2.50	2.72	2.90	3.02
$\omega_e(A^3\Pi)$, cm^{-1}	228	135	113	110
zfs, cm^{-1} [e]	5	76	218	463
$T_e(A^3\Pi_{0^+})$, cm^{-1}	24 215	22 178	21 771	25 200
$r_e(A^3\Pi_{0^+})$, Å	2.48	2.76	3.03	3.27
$\omega_e(A^3\Pi_{0^+})$, cm^{-1}	229	125	89	71
$\tau_{A^3\Pi}$, μs	0.19	0.45	0.56	2.0
$\tau_{A^3\Pi_{0^+}}$, μs	-	1.05	1.93	0.42

[a] The subscript e refers to the parameter at r_e of the corresponding state. [b] Reference 33. [c] Reference 34. [d] Reference 35. [e] Zero field splitting [$^3\Sigma^-(1X_2) - {}^3\Sigma^-(0^+X_1)$].

of two important transitions such as $A^3\Pi_{0^+}-X^3\Sigma^-_{0^+}$ and $A^3\Pi_{0^+}-X^3\Sigma^-_1$. The f values for the 0^+-0^+ transition are found to be larger than the values for the 0^+-1 transition, which makes the latter transition difficult for investigation. Although no experimental data are available as yet, these data might be useful to the experimentalists.

The dipole moments of the lowest two electronic states, namely, $X^3\Sigma^-$ and $^3\Pi$ of GaBi, are also shown in Figure 3a as a function of the bond length. Both of the curves are found to be very smooth. At the equilibrium bond length (r_e = 5.48 a_0) of the ground state, the computed dipole moments of $X^3\Sigma^-$ and $^3\Pi$ are −0.536 and −0.573 ea_0, respectively. The negative values correspond to the Ga^+Bi^- polarity. The appearance of a minimum in the dipole curve of the $^3\Pi$ state is mainly due to the avoided crossing of the potential curves of $^3\Pi$ with $2^3\Pi$ as seen in Figure 1a. It may be noted that for the $^3\Pi$ state the $\sigma'\pi^2\pi^*$ configuration starts mixing strongly with the main configuration ($\sigma'\pi^3$) at the longer bond length region. The π MO is purely nonbonding and localized on the bismuth atom, whereas π^* is an antibonding MO with its charge center away from the Bi atom. As a result, the dipole moment curve of the $^3\Pi$ state shows the minimum (Figure 3a).

Comparative Study of the Electronic Spectrum of GaX (X = P, As, Sb, Bi). Electronic structures and spectroscopic features of GaP, GaAs, and GaSb molecules are extensively studied in recent years[33−35] by using ab initio based MRDCI calculations at the same level. In this section, we shall compare different spectroscopic properties of these molecules with GaBi. Some of the computed properties of these molecules are summarized in Table 8. At the Λ-S level, the ground-state symmetries of all four gallium molecules are $X^3\Sigma^-$, which is

represented by the dominant configuration $...\sigma^2\sigma^{*2}\sigma'^2\pi^2$. The ground-state equilibrium bond lengths and vibrational frequencies follow the desired trend. As expected, r_e values increase from GaP to GaBi, whereas ω_es show the opposite trend. The $^3\Pi$ state is found to be the first excited state of all four molecules. The Ga−X bonds in the $^3\Pi$ state are consistently shorter than their ground-state bonds by 0.22−0.27 Å. This has been found to be the general feature of group III−V diatomic molecules because of the increase in delocalization through the occupancy of π molecular orbitals. The $^3\Pi$ states of these molecules are represented predominantly by $...\sigma^2\sigma^{*2}\sigma'\pi^3$. The $\Delta E(^1\Pi-^3\Pi)$ splittings of GaP and GaAs are comparable in magnitude. The smallest splitting of 4121 cm^{-1} has been noted for the heavier GaBi molecule. Potential energy curves of the low-lying Λ-S states of all four molecules are quite similar. The calculated ground-state dissociation energy (D_e) of GaBi has been found to be the smallest, and that of GaP is the largest, whereas for both GaAs and GaSb, the computed D_e values are about 1.3 eV. The experimental D_0^0 values are always found to be higher than the computed values by 0.30−0.70 eV.

The most important excited state of the group III−V molecules is $A^3\Pi$, which is the third root of the $^3\Pi$ symmetry. Only for GaAs, the A−X transition has been experimentally identified. However, the MRDCI calculations suggest that the $A^3\Pi-X^3\Sigma^-$ transition for other GaX molecules should be observed in the range 20 000−25 000 cm^{-1} as well. The smallest transition energy is noted for the heavier GaBi molecule. The r_e and ω_e values of the $A^3\Pi$ states of these four GaX molecules also show the expected trend. The A−X transitions for all four molecules are found to be strong. In the absence of the spin−orbit coupling, the radiative lifetimes of the $A^3\Pi$ state increase from GaP to GaBi. Effects of the spin−orbit coupling on the electronic spectrum are largest for GaBi. Several avoided curve crossings change the spectroscopic properties of GaBi to a larger extent in comparison to those of GaP, GaAs, and GaSb. Because it is a lighter molecule, the spectral features of GaP do not show any significant change because of the spin−orbit coupling. For GaBi, the ground-state zero-field splitting has been found to be 463 cm^{-1}, which is the largest among four gallium molecules compared here. The GaP molecule shows almost no zero-field splitting. The $\Omega = 2$, 1, and 0^- components of $A^3\Pi$ undergo predissociation for all four molecules because of their strong interactions with those of the repulsive $^5\Sigma^-$ states. Only $A^3\Pi_{0^+}$ components of these molecules survive the predissociation and form bound states from which transitions to the low-lying components with $\Delta\Lambda = 0$ and ±1 take place. The transition energy of the $A^3\Pi_{0^+}$ component of GaBi at the equilibrium bond length is somewhat larger than others because of the strongest spin−orbit coupling. Both $A^3\Pi_{0^+}-X^3\Sigma^-_{0^+}$ and $A^3\Pi_{0^+}-X^3\Sigma^-_1$ transitions are predicted to be quite strong for all four gallium molecules. In the absence of any spin−orbit coupling, the $A^3\Pi$ state of GaP has the smallest radiative lifetime, which increases with the mass of the molecule. The $A^3\Pi$ state of the GaBi molecule has the largest lifetime of 2.0 μs. However, with the inclusion of the spin−orbit coupling, the trend of the radiative lifetimes of the surviving $A^3\Pi_{0^+}$ component changes. The $A^3\Pi_{0^+}$ component of GaBi becomes shortest-lived because of the strongest spin−orbit coupling. Of the four gallium molecules, GaBi has the smallest ground-state dipole moment ($\mu = 1.29$ D) at the equilibrium bond length. It may be mentioned here that the dipole moment values for all four molecules reported in Table 8 correspond to the Ga^+-X^- polarity.

IV. Conclusion

The MRDCI calculations based on RECP have revealed the ground-state Λ-S symmetry of the GaBi molecule as $X^3\Sigma^-$ analogous to other isovalent molecules of gallium in group V such as GaP, GaAs, and GaSb. The computed ground-state r_e and ω_e of GaBi are 2.90 Å and 152 cm^{-1}, respectively. Although no experimental or theoretical spectroscopic constants of GaBi are available, the absence of d correlation and the use of RECP in the CI calculations are known to introduce some errors in the spectroscopic parameters reported here. However, a comparison among the properties of GaP, GaAs, GaSb, and GaBi shows the expected trend. The ground state is found to be composed of a dominant electronic configuration $...\sigma^2\sigma^{*2}\sigma'^2\pi^2$. There are at least 19 Λ-S states, which are bound within 46 000 cm^{-1}. The computed potential energy curves show some strongly bound quintet states above 35 000 cm^{-1}. The ground-state dissociation energy of GaBi is estimated to be 1.24 eV, which is somewhat smaller than the mass spectrometric value of 1.6 ± 0.17 eV. The discrepancy is due to the neglect of the d-electron correlation and the use of effective core potentials for Ga and Bi atoms. The transition energy of the $A^3\Pi$ state of GaBi is the lowest among other members of the group. A strong spin−orbit coupling changes the nature of potential energy curves and spectroscopic properties of Ω states of GaBi. The zero-field splitting of the ground state of GaBi is 463 cm^{-1}, which is considerably large compared with other GaX (X = P, As, Sb) molecules of group V. Most of the Λ-S states interact very strongly through the spin−orbit coupling. As a result, none of the Ω states remains pure Λ-S character. Several strong avoided crossings result many states predissociative. Like other isovalent group III−V molecules, the $A\ ^3\Pi_{0^+}$ component of GaBi survives the predissociation and becomes a suitable candidate for strong transitions to the ground-state components. The present calculations predict that $A^3\Pi_{0^+}-X^3\Sigma^-_{0^+}$, $A^3\Pi_{0^+}-X^3\Sigma^-_1$, and $A^3\Pi_{0^+}-{}^3\Pi_{0^+}$ transitions are reasonably strong to be observed experimentally. The estimated radiative lifetime of the $A\ ^3\Pi_{0^+}$ state of GaBi is 0.42 μs at the lowest vibrational level.

Acknowledgment. The authors are grateful to Prof. Dr. Robert J. Buenker, Wuppertal, Germany for his permission to use his CI codes. S.C. thanks CSIR, Government of India for the award of Junior Research Fellowship.

References and Notes

(1) O'Brien, S. C.; Liu, Y.; Zhang, Q.; Heath, J. R.; Tittel, F. K.; Curl, R. F.; Smalley, R. E. *J. Chem. Phys.* **1986**, *84*, 4074.

(2) Liu, Y.; Zhang, Q.; Tittel, F. K.; Curl, R. F.; Smalley, R. E. *J. Chem. Phys.* **1986**, *85*, 7434.

(3) Zhang, Q.; Liu, Y.; Curl, R. F.; Tittel, F. K.; Smalley, R. E. *J. Chem. Phys.* **1988**, *88*, 1670.

(4) Wang, L.; Chibante, L. P. F.; Tittel, F. K.; Curl, R. F.; Smalley, R. E. *Chem. Phys. Lett.* **1990**, *172*, 335.

(5) Jin, C.; Taylor, K.; Conciecao, J.; Smalley, R. E. *Chem. Phys. Lett.* **1990**, *175*, 17.

(6) Lou, L.; Wang, L.; Chibante, L. P. F.; Laaksonen, R. T.; Nordlanden, P.; Smalley, R. E. *J. Chem. Phys.* **1991**, *94*, 8015.

(7) Lemire, G. W.; Bishea, G. A.; Heidecke, S. A.; Morse, M. D. *J. Chem. Phys.* **1990**, *92*, 121.

(8) Arnold, C. C.; Neumark, D. M. *Can. J. Phys.* **1994**, *72*, 1322.

(9) Arnold, C. C.; Neumark, D. M. *J. Chem. Phys.* **1994**, *99*, 3353.

(10) Arnold, C. C.; Neumark, D. M. *J. Chem. Phys.* **1994**, *100*, 1797.

(11) Xu, C.; deBeer, E.; Arnold, D. W.; Arnold, C. C.; Neumark, D. M. *J. Chem. Phys.* **1994**, *101*, 5406.

(12) Burton, G. R.; Xu, C.; Arnold, C. C.; Neumark, D. M. *J. Chem. Phys.* **1996**, *104*, 2757.

(13) Van Zee, R. J.; Li, S.; Weltner, W., Jr. *J. Chem. Phys.* **1993**, *98*, 4335.

(14) Li, S.; Van Zee, R. J.; Weltner, W., Jr. *J. Chem. Phys.* **1994**, *100*, 7079.
(15) Li, S.; Van Zee, R. J.; Weltner, W., Jr. *J. Phys. Chem.* **1993**, *97*, 11393.
(16) Li, S.; Van Zee, R. J.; Weltner, W., Jr. *J. Phys. Chem.* **1994**, *98*, 2275.
(17) Piacente, V.; Desideri, A. *J. Chem. Phys.* **1972**, *57*, 2213.
(18) Balasubramanian, K. *J. Chem. Phys.* **1987**, *86*, 3410. Erratum: Balasubramanian, K. *J. Chem. Phys.* **1990**, *92*, 2123.
(19) Balasubramanian, K. *J. Mol. Spectrosc.* **1990**, *139*, 405.
(20) Balasubramanian, K. *J. Chem. Phys.* **1990**, *93*, 507.
(21) Balasubramanian, K. *Chem. Rev.* **1990**, *90*, 93.
(22) Balasubramanian, K. *Relativistic Effects in Chemistry Part A. Theory and Techniques*; Wiley-Intersciences: New York, 1997.
(23) Balasubramanian, K. *Relativistic Effects in Chemistry Part B. Applications to Molecules and Clusters*; Wiley-Intersciences: New York, 1997.
(24) Das, K. K.; Balasubramanian, K. *J. Chem. Phys.* **1991**, *94*, 6620.
(25) Feng, P. Y.; Balasubramanian, K. *Chem. Phys. Lett.* **1997**, *265*, 41.
(26) Feng, P. Y.; Balasubramanian, K. *Chem. Phys. Lett.* **1997**, *265*, 547.
(27) Feng, P. Y.; Balasubramanian, K. *Chem. Phys. Lett.* **1998**, *283*, 167.
(28) Feng, P. Y.; Balasubramanian, K. *Chem. Phys. Lett.* **1998**, *284*, 313.
(29) Meier, U.; Peyerimhoff, S. D.; Bruna, P. J.; Grein, F. *J. Mol. Spectroc.* **1989**, *134*, 259.
(30) Oranges, T.; Musolino, V.; Toscano, M.; Russo, N. *Z. Phys. D: At., Mol. Clusters* **1990**, *17*, 133.
(31) Musolino, V.; Toscano, M.; Russo, N. *J. Comput. Chem.* **1990**, *11*, 924.
(32) Toscano, M.; Russo, N. *Z. Phys. D: At., Mol. Clusters* **1992**, *22*, 683.
(33) Manna, B.; Das, K. K. *J. Mol. Struct. (THEOCHEM)* **1999**, *467*, 135.
(34) Manna, B.; Das, K. K. *J. Phys. Chem.* **1998**, *A102*, 9876.
(35) Dutta, A.; Chattopadhyay, A., and Das, K. K. *J. Phys. Chem.* **2000**, *A104*, 9777.
(36) Manna, B.; Dutta, A.; Das, K. K. *J. Phys. Chem.* **2000**, *A104*, 2764.
(37) Dutta, A.; Giri, D.; Das, K. K. *J. Phys. Chem.* **2001**, *A105*, 9049.
(38) Manna, B.; Dutta, A.; Das, K. K. *J. Mol. Struct.(THEOCHEM)* **1999**, *497*, 123.
(39) Hurley, M. M.; Pacios, L. F.; Christiansen, P. A.; Ross, R. B.; Ermler, W. C. *J. Chem. Phys.* **1986**, *84*, 6840.
(40) Wildman, S. A.; Dilabio, G. A.; Christiansen, P. A. *J. Chem. Phys.* **1997**, *107*, 9975.
(41) Buenker, R. J.; Peyerimhoff, S. D. *Theor. Chim. Acta* **1974**, *35*, 33.
(42) Buenker, R. J.; Peyerimhoff, S. D. *Theor. Chim. Acta* **1975**, *39*, 217.
(43) Buenker, R. J. *Int. J. Quantum Chem.* **1986**, *29*, 435.
(44) Buenker, R. J.; Peyerimhoff, S. D.; Butcher, W. *Mol. Phys.* **1978**, *35*, 771.
(45) Buenker, R. J. In *Proceedings of the Workshop on Quantum Chemistry and Molecular Physics;* Burton, P., Ed.; University Wollongong: Wollongong, Australia; 1980. *Studies in Physical and Theoretical Chemistry*; Carbó, R., Ed.; Elsevier: Amsterdam, 1981; Vol. 21; Current Aspects of Quantum Chemistry.
(46) Buenker, R. J.; Phillips, R. A. *J. Mol. Struct. (THEOCHEM)* **1985**, *123*, 291.
(47) Davidson, E. R. In *The World of Quantum Chemistry*; Daudel, R., Pullman, B., Eds.; Reidel: Dordrecht, The Netherlands, 1974.
(48) Hirsch, G.; Bruna, P. J.; Peyerimhoff, S. D.; Buenker, R. J. *Chem. Phys. Lett.* **1977**, *52*, 442.
(49) Cooley, J. W. *Math. Comput.* **1961**, *15*, 363.
(50) Moore, C. E. *Atomic Energy Levels*; National Bureau of Standards: Washington, DC; Vol 3.